

Octave-spanning supercontinuum generation via microwave frequency multiplication

This content has been downloaded from IOPscience. Please scroll down to see the full text.

2016 J. Phys.: Conf. Ser. 723 012035

(<http://iopscience.iop.org/1742-6596/723/1/012035>)

View [the table of contents for this issue](#), or go to the [journal homepage](#) for more

Download details:

IP Address: 132.163.81.141

This content was downloaded on 08/07/2016 at 18:05

Please note that [terms and conditions apply](#).

Octave-spanning supercontinuum generation via microwave frequency multiplication

D C Cole^{1,2,*}, K M Beha^{1,3}, S A Diddams¹ and S B Papp¹

¹Time and Frequency Division, National Institute of Standards and Technology,
325 Broadway, Boulder, CO 80305 USA

²Department of Physics, University of Colorado, Boulder, CO 80309, USA

³Current: Menlo Systems, Am Klopferspitz 19a, D-82152 Martinsried, Germany

*Corresponding author: daniel.cole@nist.gov

Abstract. We demonstrate a system based on telecom components for the generation of a coherent octave-spanning supercontinuum from a continuous-wave laser. The system utilizes direct multiplication of a 10 GHz signal derived from a commercial synthesizer to carve pulses from the laser, which are then iteratively chirped and compressed in two stages. After reducing the repetition rate of the resulting pulse train to 2.5 GHz using selective transmission through an electro-optic gate, propagation through highly-nonlinear fiber generates an octave-spanning supercontinuum spectrum. We discuss the impact of the noise of the modulation frequency on the coherence of the supercontinuum and discuss its mitigation. Close agreement between experiment and theory is shown throughout, and we use our ability to precisely model the experiment to propose an extension of the system to 20 GHz repetition rate.

The self-referenced optical frequency comb has revolutionized precision metrology and spectroscopy by providing a set of known, equidistant optical frequencies and linking these frequencies to microwave signals traceable to the SI second [1, 2]. Recently, the potential to use frequency combs for new applications and to expand their utility in present ones has driven efforts to develop combs with pulse repetition rates and mode spacings of 10 GHz and above. This is much higher than the typical 0.1-1 GHz repetition rates of most femtosecond mode-locked laser combs found in commercial production and in research labs. The applications that stand to benefit from higher repetition rates exploit individual access to widely-spaced comb modes and high power per mode, and include astronomical spectrograph calibration [3, 4], precision spectroscopy [5], optical arbitrary waveform generation [6], and optical communications [7, 8]. These applications, and in particular spectrograph calibration and precision spectroscopy, will benefit from measurement and stabilization of the comb's carrier-envelope offset frequency f_{CEO} . Due to the properties of mode-locked lasers, it has proven challenging to build mode-locked laser combs operating above 10 GHz repetition rate for which f_{CEO} can be detected [9]. Thus, there is a need for new means to provide high repetition rate trains of short, high peak power pulses for generation of octave-spanning optical spectra and $f - 2f$ interferometry.

One method for generation of high-repetition-rate pulse trains is the electro-optic modulation (EOM) comb scheme [10-14]. In this scheme, a microwave frequency input is multiplied through the generation of many intensity- and phase-modulation sidebands on a continuous-wave (CW) seed laser, yielding a pulse train in the time domain. This multiplication can be continued through subsequent nonlinear



spectral broadening of the pulses. For the case of octave-spanning supercontinuum spectra, the multiplication factor is ultimately on the order of the ratio of the CW laser's optical frequency to the microwave modulation frequency – for the 10 GHz system discussed here the factor is 19340.

The EOM comb scheme for comb generation has advantages in the flexibility of the comb's repetition rate f_r , the fast and independent tunability of the repetition rate and seed frequency for any particular comb, the flatness of the initial comb's spectrum, and the compressibility of the comb's pulses. Recently, we demonstrated self-referencing of an EOM comb system with 10 GHz repetition rate and measured the frequency of the comb's CW seed laser to a stability beyond 5 parts in 10^{14} [15]. In this proceeding, we discuss in detail our 10 GHz EOM comb system and demonstrate that it may be precisely modelled with a side-by-side comparison of experimental and calculated spectra. We also discuss a unique challenge in using the EOM comb scheme to generate a coherent octave-spanning supercontinuum, which is the linearly increasing contribution of the frequency noise of the modulation tone from which f_r is derived to the frequency fluctuations of the optical comb modes. Finally, we propose a simplification and an extension of our 10 GHz system to 20 GHz repetition rate and beyond.

The experimental system we discuss here is shown in figure 1a. In order to generate the short optical pulses required for coherent supercontinuum generation in highly-nonlinear fiber (HNLF), our system consists of several stages. In the first stage, an intensity modulator carves 50 % duty cycle optical pulses from a fiber-coupled 1550 nm CW seed laser and the pulses are chirped using two LiNbO₃ phase modulators, then the pulses are temporally compressed in single-mode fiber (SMF). In the second stage, the pulses are amplified in an erbium-doped fiber amplifier (EDFA), chirped again via self-phase modulation (SPM) in 100 m of HNLF (see e.g. Ref. 16 for previous work using this technique), and temporally compressed using a spatial light modulator (SLM). In the final stage, the pulse repetition rate may be reduced with an electro-optic gate, after which the pulses are amplified and launched into hybrid HNLF for generation of an octave-spanning supercontinuum spectrum. Also included in our system in the second stage is an optical Fabry-Perot filter cavity for the purpose of reducing the impact of the frequency noise of the modulation tone; this is discussed in detail below.

To introduce the EOM comb system, we present a standard calculation of the comb's electric field following intensity and phase modulation for generation of the initial chirped pulse train. The seed laser's field $E_0 e^{i\omega_c t}$ is multiplied by factors $\frac{1}{2} \left[1 + \exp \left(i \frac{\pi}{2} (1 + \sin \omega_r t) \right) \right]$ and $\exp(i\beta_m \sin \omega_r t)$, which result respectively from 50 % duty-cycle intensity modulation and phase modulation with modulation index β_m at the angular frequency $\omega_r = 2\pi f_r$. Up to an overall optical phase shift and a shift in time, the resulting field is:

$$E = E_0 \times \cos \left[\frac{\pi}{2} \sin^2(\omega_r t / 2) \right] \times \exp \left[i\omega_c t - i \left(\beta_m + \frac{\pi}{4} \right) \cos \omega_r t \right]. \quad (1)$$

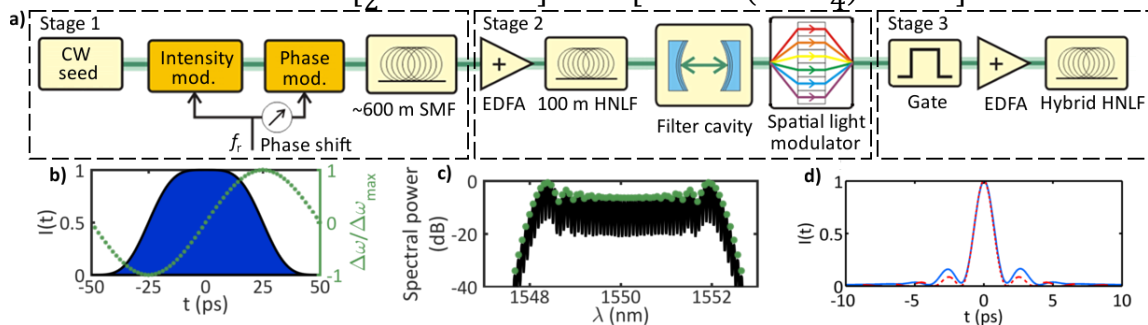


Figure 1 (colour online). (a) Experimental apparatus for generation of octave-spanning supercontinuum from a CW laser. (b) Relation between intensity profile (solid blue) and instantaneous carrier frequency (dotted green) of the initial chirped pulses generated by the EOM comb scheme after intensity and phase modulation. (c) A comparison of the experimental spectrum of the EOM comb (black) to a calculation of the spectrum (green circles). (d) Calculations of the temporal intensity profile of the EOM comb pulses after compression in 570 m SMF (solid blue) and for perfect compression to the Fourier-transform limit (dashed red). Full-width at half maximum (FWHM) of both traces is ~ 1.5 ps.

This can be understood as the product of a time-varying real amplitude and a phase factor from which the instantaneous carrier frequency $\omega_c + \Delta\omega(t)$ can be calculated: $\Delta\omega(t) = \omega_r \left(\beta_m + \frac{\pi}{4} \right) \sin \omega_r t$. The pulse intensity and the oscillating carrier frequency are plotted in figure 1b. The carrier frequency of the pulses increases in time, permitting pulse compression in standard anomalously dispersive SMF. Additionally, the range of instantaneous carrier frequencies $\omega_c + \Delta\omega(t)$ occurring during the flat top of the intensity profile shown in figure 1b is represented with equal weight in the optical spectrum of the pulse train, yielding a wide, flat central feature in the spectrum. The phase-modulation index sets the optical bandwidth. A comparison between the measured spectrum of our EOM comb and a calculation using $\beta_m = 15\pi/2$ is shown in figure 1c.

After generation of the EOM comb, we propagate the pulse train through ~ 600 m of SMF for pulse compression. Simulated results of this compression are shown in figure 1d, and indicate that compression to near the Fourier transform limit is possible. Intuitively, this is because components of the pulse occurring later in time have higher carrier frequency and propagate more quickly than components occurring earlier. The resulting ~ 1.5 ps duration of the pulses enables efficient generation of SPM chirp in the second stage of the experiment. After amplification to 400 mW average power, the pulses are launched into 100 m of low-dispersion HNLF. The specified dispersion values at 1550 nm are $D = -0.04$ ps/nm · km and $D' = 0.01$ ps/nm² · km, and SPM dominates the pulse-evolution dynamics [17]. The SPM chirp increases the 4 nm initial bandwidth of the pulses to ~ 40 nm, in good agreement with a numerical simulation, as shown in figure 2a. We perform the simulation using the non-linear Schrödinger equation (NLSE) including 3rd-order dispersion, taking as initial conditions the calculated intensity profile of the EOM comb pulses after compression in 570 m SMF (blue trace in figure 1d). The dispersion values for the HNLF used in the simulation are $D = -0.04$ ps/nm · km and $D' = 0.003$ ps/nm² · km, close to the values specified by the manufacturer.

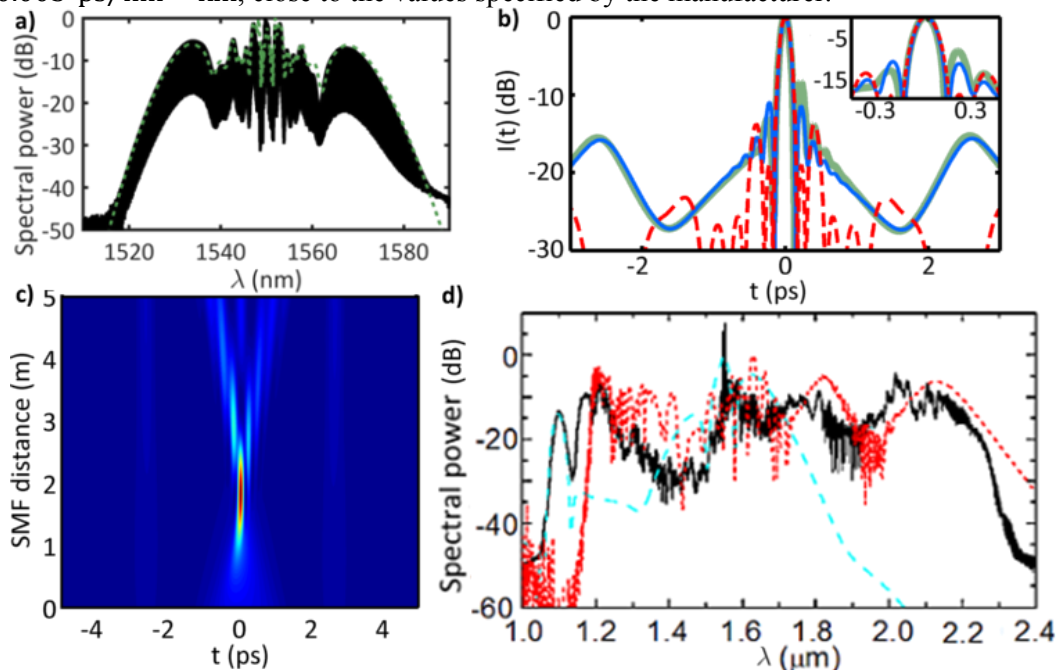


Figure 2 (colour online). (a) Comparison of experiment (black) with simulation (dotted green) for the spectrum after SPM. (b) Logarithmic-scale plot of simulations of SLM-compressed (blue), SMF-compressed (thick green) and transform-limited (dashed red) intensity profiles corresponding to the simulated spectrum in (a). Asymmetry in the SMF-compressed pulse is due to higher order dispersion. Inset: the same, plotted to emphasize the asymmetry. (c) Simulated compression of the SPM-chirped pulses during propagation in SMF. (d) Experimental octave-spanning supercontinuum generated by the EOM comb system (black), plotted with simulated spectra resulting from propagation in the first, 30 cm section (long-dashed teal) and the second, 7.7 m section (short-dashed red) of the hybrid HNLF.

After generation of the SPM chirp, the pulses are transmitted through a Fabry-Perot cavity for suppression of optical frequency fluctuations, as we will discuss below. We then pass the pulse train through an SLM, which provides direct control of each comb mode's optical phase. Using the SLM, we iteratively adjust the pulse train's 2nd-, 3rd-, and 4th-order chirp to compress the pulses. Figure 2b shows a calculation of the pulse intensity profile which would result from complete removal of 2nd- to 4th-order chirp after propagation in the HNLF, as well as fully compressed pulses with flat spectral phase. Both intensity profiles have pulse widths of 130 fs, but the intensity profile compressed by the SLM has a substantial fraction of its energy in satellite pulses at ± 2.5 ps with respect to the central pulse. This is due to higher-order chirp. We note that the SLM is convenient but not necessary – numerical simulations indicate that the SPM chirp can be compressed in an appropriate length of SMF by the same mechanism as the chirp imposed by external phase modulation, as discussed above. Results of a simulation of this compression employing the NLSE with Kerr nonlinearity and the full specified dispersion curve for SMF are also shown in figure 2b; after propagation through 1.8 m of SMF, the pulses reach 130 fs duration with satellite pulses at ± 2.5 ps, similar to what can be achieved using the SLM as described above. The pulse evolution during propagation in SMF is shown in figure 2c.

In the third stage of the experiment, after pulse compression in the SLM, the pulses are passed through a Mach-Zehnder modulator functioning as an electro-optic gate. The gate is used to selectively transmit pulses and reduce the pulse repetition rate [18, 19]. This facilitates supercontinuum generation by increasing the pulse train's peak-to-average power ratio. While we have shown in Ref. 15 that a coherent octave-spanning supercontinuum may be generated without the gate by amplifying to an average power of 4 W, here we focus on the case where the repetition rate is reduced to 2.5 GHz.

The 2.5 GHz pulse train is amplified to 1.4 W average power and passed through 8 m of hybrid HNLF, yielding the spectrum shown in figure 2d. The hybrid HNLF consists of two sections of fiber with different dispersion characteristics, and we can qualitatively understand the supercontinuum spectrum by considering the two sections independently [20]. The first fiber is 30 cm of highly dispersive HNLF ($D = 6$ ps/nm · km), and generates a dispersive wave centered at 1090 nm. Simulated results of propagation in this fiber are shown in teal in figure 2d. The second fiber is 7.7 m of lower dispersion HNLF ($D = 1.5$ ps/nm · km), and generates a Raman-self-frequency-shifted soliton centered near 2150 nm. Simulated results of propagation in this fiber are shown in red. Simulations use the LaserFOAM program [21], which employs the generalized NLSE including Raman scattering, self-steepening, and 2nd- to 4th-order dispersion. The two simulations are run independently, and both take as initial conditions 170 fs Gaussian pulses with 350 pJ energy, close to the energy remaining in the pulses exiting the amplifier after accounting for loss between the amplifier and the HNLF.

For the octave-spanning supercontinuum generated in the HNLF to be useful it must be coherent, with resolvable comb modes. The contribution of the noise of the modulation tone f_r to the optical frequency noise of the comb modes scales linearly with mode number N , as measured relative to the seed laser; the contribution to the power spectrum of frequency noise scales as N^2 . This presents a challenge for maintaining coherence of the supercontinuum and detecting f_{CEO} . For standard $f - 2f$ interferometry, the factor by which the noise of f_r is multiplied to determine its contribution to the f_{CEO} signal is the ratio between the seed frequency and the repetition rate; $N = f_c/f_r = 19340$ for the 10 GHz comb discussed here. This contribution is shown in figure 3a, along with the contribution from the CW seed laser. The noise on f_r is determined by the technical noise from the synthesizer at low Fourier frequencies and approaches a white Johnson-Nyquist phase noise floor of -177 dBm/Hz at high Fourier frequencies. As discussed in Ref. 15, unmitigated multiplication of the white phase noise floor by 19340 leads to frequency fluctuations that are high enough to prevent detection and measurement of f_{CEO} . By passing the pulse train through a Fabry-Perot cavity whose free spectral range is actively stabilized to the comb's mode spacing, the contribution of the Johnson-Nyquist frequency noise at high Fourier frequencies is reduced by the filter cavity's Lorentzian transfer function, leading to resolvable comb modes in the supercontinuum and permitting measurement of f_{CEO} . We use a filter cavity with 7.5 MHz

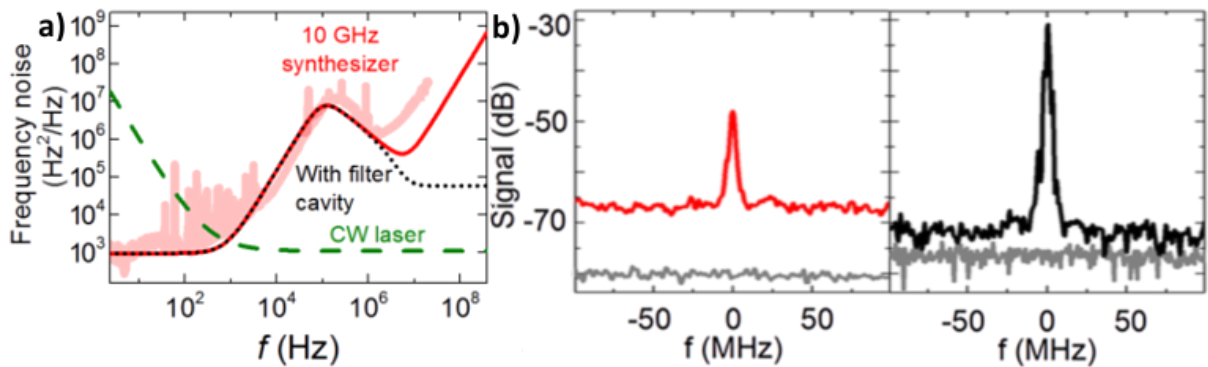


Figure 3 (colour online). (a) Contributions to the spectrum of frequency fluctuations of the carrier-envelope offset frequency detected through $f - 2f$ interferometry: model of the CW laser (dashed green), model of the 10 GHz synthesizer multiplied by 19340^2 without filter cavity (solid red, experimental data thick red), and synthesizer multiplied by 19340^2 and the filter cavity transfer function (dotted black). (b) A comparison of detected heterodyne beats between the supercontinuum and a 1319 nm wavelength CW laser without (red, left) and with (black, right) the optical filter cavity. The level of intensity noise on the supercontinuum, measured by removing the 1319 nm CW laser, is shown by the lower gray trace in each plot. Signal-to-noise ratios for the beat are 17 dB without and 40 dB with the filter cavity.

linewidth. The effect of the cavity is shown concretely in figure 3b, where we compare the lineshape of a heterodyne beat between the supercontinuum and a CW laser with 1319 nm wavelength without filter cavity and with the cavity in place. The signal-to-noise ratios for the beat without the cavity and with it are 17 dB and 40 dB, respectively.

Lastly, we propose a simplification and extension of this system to 20 GHz repetition rate, and possibly beyond. The initial bandwidth of an EOM comb scales with the comb's mode spacing and with the phase-modulation index β_m , which determines the number of modes generated. By modestly increasing both parameters, the spectral broadening for supercontinuum generation can be accomplished in a single piece of fiber because sufficiently short (several hundred femtoseconds) optical pulses are supported by the initial comb spectrum. The system we propose is shown in figure 4a, where four phase modulators are used with an intermediate booster amplifier to achieve a phase-modulation index of $\beta_m = 45\pi/2$. The calculated bandwidth for this comb is 25 nm, and the simulated spectrum is shown in blue

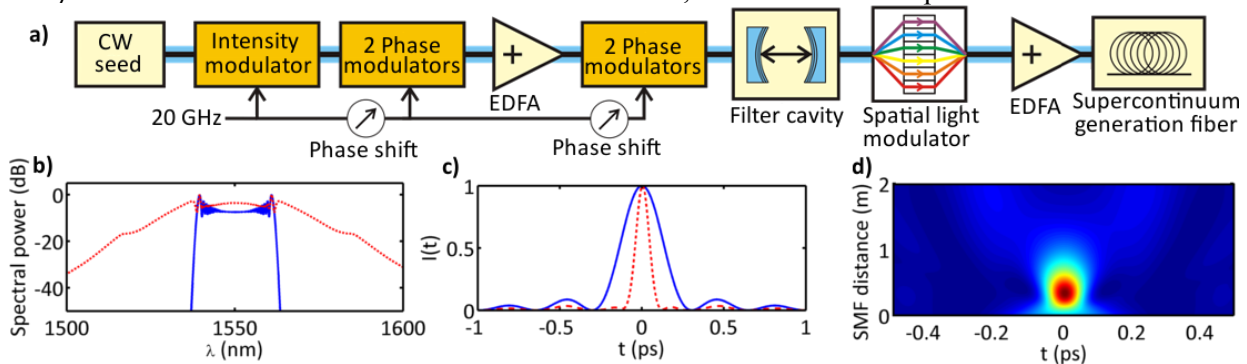


Figure 4 (colour online). (a) Proposed experimental setup for generation of ~ 100 fs pulses to seed supercontinuum generation at a 20 GHz repetition rate. (b) Calculations of the EOM comb spectrum at 20 GHz with $\beta_m = 45\pi/2$ (solid blue) and the SPM-broadened spectrum after propagation in 20 cm of low-dispersion HNLF at 8 W average power (dotted red). (c) Time-domain intensity profiles corresponding to the spectra in (b). The trace for the SPM-broadened spectrum includes pulse compression in an appropriate length of SMF, with a resulting pulse width of 92 fs. (d) Simulated compression of the pulses in SMF after SPM chirp-generation in 20 cm of HNLF.

in figure 4b. After passing the pulse train through the filter cavity for suppression of frequency fluctuations, we can exploit our precise modelling of the EOM comb to use the SLM to compress the pulses to the transform-limited duration of 275 fs. Using a commercially available 10 W EDFA, the pulses can be amplified to 500 pJ energy and launched into a piece the low-dispersion HNLF, with the resulting spectrum plotted in figure 4b. After propagation through an appropriate length of SMF for pulse compression, pulses with 92 fs FWHM duration result, as shown in figure 4c. A simulation of the compression of the pulses in SMF including both nonlinearity and dispersion is shown in figure 4d. We expect the compressed, ~350 pJ pulses to generate coherent octave-spanning supercontinuum in the hybrid HNLF, in accordance with our results presented above.

Our system provides a simple and direct route to octave-spanning supercontinuum at 2.5 GHz and 10 GHz repetition rates. In Ref. 15, we have demonstrated that spectra generated with this technique are coherent and suitable for optical frequency metrology. The comb's wide mode spacing and the tunability of the comb's repetition rate and offset frequency, via tuning of the comb's seed laser, make the system ideal for optical arbitrary waveform generation, astronomical spectrograph calibration, and fast acquisition of precise spectroscopic data. The extension of this technique to higher repetition rates is limited largely by the challenge of achieving high pulse train average power for nonlinear spectral broadening and by the availability of stable microwave sources for generation of the modulation tone. Finally, we emphasize that this system has the advantage of being well understood and amenable to precise numerical modelling, and that the EOM comb system can be constructed from commercially available parts using mature technology from the telecom industry.

We thank Travis Briles and Tara Drake for helpful comments on the manuscript and M. Hirano for providing the HNLF. This work is supported by the DARPA QuASAR program, AFOSR, NASA, and NIST. DC acknowledges support from the NSF GRFP under Grant No. DGE 1144083. This work is a contribution of the US government and is not subject to copyright in the United States.

References

- [1] Udem T, Holzwarth R, and Hansch T 2002 *Nature* **416** 233
- [2] Diddams S 2010 *Journal of the Optical Society of America B* **27** B51
- [3] Steinmetz T *et al.* 2008 *Science* **321** 1335
- [4] Ycas G *et al.* 2012 *Optics Express* **20** 6631
- [5] Stowe M *et al.* 2008 *Advances in Atomic, Molecular, and Optical Physics* **55** 1
- [6] Jiang Z, Huang C-B, Leaird D and Weiner A 2007 *Nature Photonics* **1** 463
- [7] Ellis A and Gunning F 2005 *Photonics Technology Letters* **17** 504
- [8] Delfyett P *et al.* 2006 *Journal of Lightwave Technology* **24** 2701
- [9] Bartels A, Heinecke D and Diddams S 2009 *Science* **326** 681
- [10] Murata H *et al.* 2000 *IEEE Journal of Selected Topics in Quantum Electronics* **6** 1325
- [11] Metcalf A *et al.* 2013 *IEEE Journal of Selected Topics in Quantum Electronics* **19** 3500306
- [12] Ishizawa A *et al.* 2010 *Electronics Letters* **36** 1343
- [13] Wu R, Supradeepa V, Long C, Leaird D and Weiner A 2010 *Optics Letters* **35** 3234
- [14] Wu R, Torres-Company V, Leaird D and Weiner A 2013 *Optics Express* **21** 6045
- [15] Beha K *et al.* *Preprint* arXiv:1507.06344
- [16] Myslivets E, Kuo B, Alic N and Radic S 2012 *Optics Express* **20** 3331
- [17] Agrawal G 2007 *Nonlinear Fiber Optics* (Burlington: Academic Press)
- [18] Cole D, Papp S and Diddams S 2013 *Preprint* arXiv:1310.4134
- [19] Mandridis D *et al.* 2010 *Applied Optics* **49** 2850
- [20] Dudley J, Genty G and Coen S 2006 *Reviews of Modern Physics* **78** 1135
- [21] Amorim A *et al.* 2009 *Optics Letters* **34** 3851